Wind and Structures, Vol. 1, No. 2 (1998) 161-174
DOI: http://dx.doi.org/10.12989/was.1998.1.2.161

Generalized equivalent spectrum technique

G. Piccardo† and G. Solari‡

DISEG, Department of Structural and Geotechnical Engineering,
University of Genova, Via Montallegro 1, 16145 Genova, Italy

Abstract. Wind forces on structures are usually schematized by the sum of their mean static part and a nil mean fluctuation generally treated as a stationary process randomly varying in space and time. The multi-variate and multi-dimensional nature of such a process requires a considerable quantity of numerical procedures to carry out the dynamic analysis of the structural response. With the aim of drastically reducing the above computational burden, this paper introduces a method by means of which the external fluctuating wind forces on slender structures and structural elements are schematized by an equivalent process identically coherent in space. This process is identified by a power spectral density function, called the Generalized Equivalent Spectrum, whose expression is given in closed form.

Key words: atmospheric turbulence; coherence; dynamic response; equivalent spectrum; multi-dimensional process; multi-variate process; wind loading.

1. Introduction

Wind action is usually schematized by a suitable distribution of forces applied on the structural surface. These forces are represented by the sum of their mean static part and a nil mean fluctuation generally treated as a stationary process randomly varying in space and time and schematized, in the frequency domain, by its cross-power spectral density function (cpsdf). This function represents the input quantity for analyzing the dynamic response of structures both in the frequency and in the time domain.

Assuming that the structure is a linear elastic system, its dynamic analysis is carried out by projecting the external forces over the dominant modes. Since the loading process is characterized by a low frequency harmonic content, only the contribution of the fundamental mode is usually retained. In other words, working in the frequency domain, the cpsdf of the loading process is transformed into the power spectral density function (psdf) of the first modal force which, from then on, collects all the information concerning the wind and its action (Solari 1994). This operation is often the most burdensome step of the whole calculation procedure.

On the other hand, solving the problem in the time domain, independently of the structural properties, the cpsdf of the external forces is first of all utilized in order to obtain, through a Monte Carlo procedure, a suitable set of cross-correlated artificial loading time histories (Di Paola 1998). Whenever they are used in the following steps of the analysis, their generation represents one of the most burdensome phases of the whole numeric development.

† Assistant Professor
‡ Professor

In order to drastically reduce the above computational effort, the authors of this paper proposed a method (Piccardo and Solari 1996b), namely the Equivalent Wind Loading Spectrum Technique (EWLST), aimed at schematizing the fluctuating alongwind, crosswind and torsional generalized wind forces, on slender structures and structural elements by a fictitious equivalent process identically coherent in space rather than by the actual cross-correlated process. This process was identified by a psdf, the Equivalent Wind Loading Spectrum (EWLS), whose expression was given in closed form. The EWLS gave rise to a first modal force whose psdf is the same as that obtained applying the cpsdf of the actual wind loading over the structure.

The present paper recalls and generalizes the previous method by taking into account some new features among which, primarily, the cross-correlation of the longitudinal and vertical turbulence. The generalized psdf of the modified equivalent process is called the Generalized Equivalent Spectrum (GES) and its application is referred to as the Generalized Equivalent Spectrum Technique (GEST).

Due to the above prerogatives, the GEST represents the full extension, at present limited to slender structures and structural elements, of the Equivalent Wind Spectrum Technique (EWST) (Solari 1988) from the alongwind gust buffeting to the 3-D wind loading of structures.

2. Wind loading model

Consider a slender cylinder of finite length l representing a structure or a structural element in the atmospheric boundary layer. Let x, y, z be a local Cartesian reference system with origin at o; z coincides with the axis of the cylinder, x is aligned with the mean wind direction, o lies on the face of the cylinder with z=0, at height h over the ground.

Let X, Y, Z be a global Cartesian reference system with origin at O; X, Y axes are coplanar with ground; Y, Z are coplanar with y, z; X is parallel to x; Z is directed upwards and passes through O; z is rotated ϕ with respect to Z (Fig. 1). Let u be the mean wind velocity aligned with X, x; u', v', w' are the longitudinal (X, x), lateral (Y) and vertical (Z) nil mean turbulent fluctuations, treated here as stochastic stationary Gaussian processes, assuming that $u'/\bar{u} << 1$, $v'/u << 1$, $w'/\bar{u} << 1$ (Davenport 1961). Coherently with ESDU (1990b) the u', w' turbulence components are cross-correlated, while the correlation of the u', v' and v', w' turbulence components is considered as negligible.

The wind loading is schematized by a three-dimensional stochastic process, whose α-th component (α=x, y, θ) is expressed by :

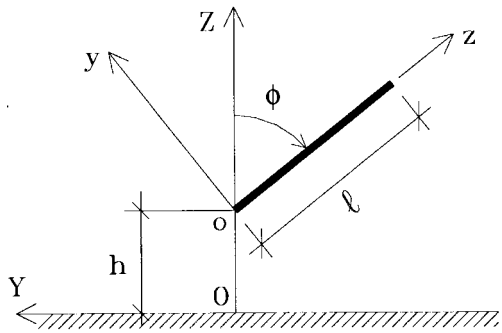

Fig. 1 Structural model and reference systems (X, x entering the page)

$$F_\alpha(z\,;t)=\bar{F}_\alpha(z)+F'_\alpha(z\,;t) \tag{1}$$

where t is the time; $\bar{F}_\alpha$ is the mean value of F_α; F'_α is the nil mean fluctuation of F_α around $\bar{F}_\alpha$; F_x, F_y, F_θ are the alongwind force, the crosswind force and the torsional moment, respectively.

Using the model proposed by Piccardo and Solari (1996a), F_α, F'_α are given by

$$F_\alpha(z)=\frac{1}{2}\rho u^2(z)\,b\,\lambda_\alpha c_{\alpha u}\,\gamma_{\alpha u}(z) \tag{2}$$

$$F'_\alpha(z\,;t)=\sum\nolimits_\varepsilon F'_{\alpha\varepsilon}(z\,;t) \tag{3}$$

$$F'_{\alpha\varepsilon}(z\,;t)=c_{\alpha\varepsilon}\,\bar{f}_{\alpha\varepsilon}(z)\,f^*_{\alpha\varepsilon}(z\,;t) \tag{4}$$

$$\bar{f}_{\alpha\varepsilon}(z)=\frac{1}{2}\rho\bar{u}^2(z)\,b\,\lambda_\alpha\gamma_{\alpha\varepsilon}(z)J_\varepsilon(z) \tag{5}$$

where ρ is the air density; b is a reference size of the cylinder section; Σ_ε is the sum of four ordered terms with indices $\varepsilon=u,\ v,\ w,\ s$; $F'_{\alpha u}$, $F'_{\alpha v}$, $F'_{\alpha w}$, $F'_{\alpha s}$ are the components of F'_α associated with the three turbulence components (u, v, w) and the vortex shedding (s); λ_α, $c_{\alpha\varepsilon}$, J_ε, $f^*_{\alpha\varepsilon}$ are the α, ε components ($\alpha=x,\ y,\ \theta$; $\varepsilon=u,\ v,\ w,\ s$) of the following vectors and matrices :

$$\{\lambda\}=\{\lambda_x\ \lambda_y\ \lambda_\theta\}^T=\{1\ \ 1\ \ b\}^T \tag{6}$$

$$[c]=\begin{bmatrix} c_d & (c'_d-c_l)\cos\phi & (c'_d-c_l)\sin\phi & \tilde{c}_{ds} \\ c_l & (c_d+c'_l)\cos\phi & (c_d+c'_l)\sin\phi & \tilde{c}_{ls} \\ c_m & c'_m\cos\phi & c'_m\sin\phi & \tilde{c}_{ms} \end{bmatrix} \tag{7}$$

$$\{J(z)\}=\{2I_u(z)\ \ I_v(z)\ \ I_w(z)\ \ 1\}^T \tag{8}$$

$$[f^*(z\,;t)]=\begin{bmatrix} u^*(z\,;t) & v^*(z\,;t) & w^*(z\,;t) & s^*_x(z\,;t) \\ u^*(z\,;t) & v^*(z\,;t) & w^*(z\,;t) & s^*_y(z\,;t) \\ u^*(z\,;t) & v^*(z\,;t) & w^*(z\,;t) & s^*_\theta(z\,;t) \end{bmatrix} \tag{9}$$

c_d, c_l, c_m are the reference drag, lift and torsional moment coefficients of the cylinder; c'_d, c'_l, c'_m are the prime angular derivatives of c_d, c_l, c_m; $\tilde{c}_{ds}$, $\tilde{c}_{ls}$, $\tilde{c}_{ms}$ are the reference root mean square (rms) drag, lift and torsional moment wake coefficients; $I_u=\sigma_u/\bar{u}$, $I_v=\sigma_v/u$, $I_w=\sigma_w/u$ are the longitudinal, lateral and vertical turbulence intensities, σ_u, σ_v, σ_w being the rms values of u', v', w'; $u^*=u'/\sigma_u$, $v^*=v'/\sigma_v$, $w^*=w'/\sigma_w$ are the reduced turbulence components; s^*_α is the α-th reduced component (with unit rms value) of the wake excitation, treated as a stochastic stationary Gaussian process uncorrelated with u^*, v^*, w^* (Solari 1985); $\gamma_{\alpha\varepsilon}$ is a non-dimensional function of z, called shape function, which makes the model suitable for ap-

plication both to elements with variable aerodynamic properties and to non-prismatic elements.

Since F_α is a linear function of $f^*_{\alpha\varepsilon}$ (Eqs. (1)-(5)), as is $f^*_{\alpha\varepsilon}$, also F_α is a stochastic stationary Gaussian process. By virtue of Eqs. (3) and (4) the cpsdf of F'_α is given by :

$$S_{F\alpha}(z, z'; n) = \sum_\varepsilon \sum_\eta S_{F\alpha\varepsilon\eta}(z, z'; n) \tag{10}$$

$$S_{F\alpha\varepsilon\eta}(z, z'; n) = c_{\alpha\varepsilon} c_{\alpha\eta} \bar{f}_{\alpha\varepsilon}(z)\, \bar{f}_{\alpha\eta}(z') S^*_{\alpha\varepsilon\eta}(z, z'; n) \tag{11}$$

$$S^*_{\alpha\varepsilon\eta}(z, z'; n) = \mathrm{Sgn}(S^*_{\alpha\varepsilon\eta}) \sqrt{S^*_{\alpha\varepsilon\eta}(z; n) S^*_{\alpha\varepsilon\eta}(z'; n)}\, \mathrm{Coh}_{\alpha\varepsilon\eta}(z, z'; n) \tag{12}$$

where n is the frequency; Σ_η, as well as Σ_ε, is the sum of four ordered terms with indices $\eta = u, v, w, s$; $S_{F\alpha\varepsilon\eta}(z, z'; n)$ is the cpsdf of $F'_{\alpha\varepsilon}(z; t)$, $F'_{\alpha\eta}(z'; t)$; $S^*_{\alpha\varepsilon\eta}(z, z'; n)$ is the cpsdf of $f^*_{\alpha\varepsilon}(z; t)$, $f^*_{\alpha\eta}(z'; t)$; $S^*_{\alpha\varepsilon\eta}(z; n) = S^*_{\alpha\varepsilon\eta}(z, z; n)$ is the cpsdf of $f^*_{\alpha\varepsilon}(z; t)$, $f^*_{\alpha\eta}(z; t)$; Sgn is the sign function; $\mathrm{Coh}_{\alpha\varepsilon}$ is the coherence function of $f^*_{\alpha\varepsilon}(z; t)$, $f^*_{\alpha\eta}(z'; t)$.

Using a definition widely applied in the technical literature :

$$\mathrm{Coh}_{\alpha\varepsilon\eta}(z, z'; n) = \exp\left\{ -\kappa_{\alpha\varepsilon\eta}(z, z'; n) \frac{|z - z'|}{l} \right\} \tag{13}$$

$\kappa_{\alpha\varepsilon\eta}$ being a non-dimensional function of z, z', n such as $\kappa_{\alpha\varepsilon\eta} \neq 0$ for $z = z'$. It is referred to as the coherence factor.

3. Generalized equivalent spectrum

Consider the structure or structural element shown in Fig. 1. Assume that it possesses three uncoupled components of motion, the alongwind and crosswind displacements respectively directed towards x, y and θ torsional rotation around z. Each $\alpha = x, y, \theta$ component of motion is considered to be only dependent on the contribution of the related fundamental mode shape $\psi_{\alpha 1}(z)$.

The psdf of the first α-th modal force is given by :

$$S_{F\alpha 1}(n) = \int_0^l \int_0^l S_{F\alpha}(z, z'; n)\, \psi_{\alpha 1}(z)\, \psi_{\alpha 1}(z')\, dz dz' \tag{14}$$

Replacing Eq. (10) into Eq. (14) it follows that :

$$S_{F\alpha 1}(n) = \sum_\varepsilon \sum_\eta c_{\alpha\varepsilon} c_{\alpha\eta} \left[\int_0^l \bar{f}_{\alpha\varepsilon}(z)\, \psi_{\alpha 1}(z)\, dz \right] \left[\int_0^l f_{\alpha\eta}(z)\, \psi_{\alpha 1}(z)\, dz \right] I_{\alpha\varepsilon\eta}(n) \tag{15}$$

where :

$$I_{\alpha\varepsilon\eta}(n) = \frac{\int_0^l \int_0^l \bar{f}_{\alpha\varepsilon}(z)\, f_{\alpha\eta}(z') S^*_{\alpha\varepsilon\eta}(z, z'; n)\, \psi_{\alpha 1}(z)\, \psi_{\alpha 1}(z')\, dz dz'}{\left[\int_0^l \bar{f}_{\alpha\varepsilon}(z)\, \psi_{\alpha 1}(z)\, dz \right] \left[\int_0^l \bar{f}_{\alpha\eta}(z')\, \psi_{\alpha 1}(z')\, dz' \right]} \tag{16}$$

is the most burdensome quantity to be determined. Its complexity is due to the multi-dimensional

nature of the cross-correlated processes $f^*_{\alpha\varepsilon}(z;\, t)$, $f^*_{\alpha\eta}(z';\, t)$, and to the related dependence of $S^*_{\alpha\varepsilon\eta}$ on z, z'.

Starting from this observation the present paper replaces the actual multi-dimensional processes $f^*_{\alpha\varepsilon}(z;\, t)$, $f^*_{\alpha\eta}(z';\, t)$, with cpsdf $S^*_{\alpha\varepsilon\eta}(z,\, z';\, n)$, by a set of equivalent mono-dimensional processes $f^*_{\alpha\varepsilon eq}(t)$, $f^*_{\alpha\eta eq}(t)$ with cpsdf $S^*_{\alpha\varepsilon\eta eq}(n)$. The cpsdf $S^*_{\alpha\varepsilon\eta eq}$ is the reduced α, ε, η component of the GES and is determined by the condition :

$$S^*_{\alpha\varepsilon\eta eq}(n) = I_{\alpha\varepsilon\eta}(n) \tag{17}$$

In particular, for $\varepsilon=\eta$, $S^*_{\alpha\varepsilon\varepsilon eq}(n)$ is the psdf of $f^*_{\alpha\varepsilon eq}(t)$ and represents the reduced α, ε component of the EWLS (Piccardo and Solari 1996b). For $\varepsilon=\eta=u$ and $\alpha=x$, $S^*_{xuu\, eq}(n)$ is the psdf of $f^*_{xu\, eq}(t)$ and represents the reduced x, u component of the EWS (Solari 1988).

Let $z_{\alpha\varepsilon\eta}$ be a constant value of z in the range 0 to l. In the limit case in which $u(z)=\bar{u}(z_{\alpha\varepsilon\eta})$, $J_\varepsilon(z)=J_\varepsilon(z_{\alpha\varepsilon\eta})$, $\gamma_{\alpha\varepsilon}(z)=\gamma_{\alpha\varepsilon}(z_{\alpha\varepsilon\eta})$, i.e. $\bar{f}_{\alpha\varepsilon}(z)=\bar{f}_{\alpha\varepsilon}(z_{\alpha\varepsilon\eta})$, and moreover $\psi_{\alpha 1}(z)=\psi_{\alpha 1}(z_{\alpha\varepsilon\eta})$, $S^*_{\alpha\varepsilon\eta}(z;\, n)=S^*_{\alpha\varepsilon\eta}(z_{\alpha\varepsilon\eta};\, n)$, $\kappa_{\alpha\varepsilon\eta}(z,\, z';\, n)=\kappa_{\alpha\varepsilon\eta}(z_{\alpha\varepsilon\eta},\, z_{\alpha\varepsilon\eta};\, n)$, it follows that :

$$S^*_{\alpha\varepsilon\eta eq}(n) = S^*_{\alpha\varepsilon\eta}(z_{\alpha\varepsilon\eta};\, n)\, \chi_{\alpha\varepsilon\eta}(z_{\alpha\varepsilon\eta};\, n) \tag{18}$$

where :

$$\chi_{\alpha\varepsilon\eta}(z_{\alpha\varepsilon\eta};\, n) = \frac{1}{l^2}\int_0^l\int_0^l \exp\left\{-\kappa_{\alpha\varepsilon\eta}(z_{\alpha\varepsilon\eta},\, z_{\alpha\varepsilon\eta};\, n)\,\frac{|z-z'|}{l}\right\} dzdz' \tag{19}$$

Solving this integral in closed form (Vellozzi and Cohen 1968) :

$$\chi_{\alpha\varepsilon\eta}(z_{\alpha\varepsilon\eta};\, n) = C\{k_{\alpha\varepsilon\eta}\,\kappa_{\alpha\varepsilon\eta}(z_{\alpha\varepsilon\eta},\, z_{\alpha\varepsilon\eta};\, n)\} \tag{20}$$

$$C\{\omega\} = \frac{1}{\omega} - \frac{1}{2\omega^2}(1-e^{-2\omega}) \quad \text{for} \quad \omega>0;\; C\{0\}=1 \tag{21}$$

where $k_{\alpha\varepsilon\eta}=0.5$.

Let us now consider a horizontal structure ($\phi=\pi/2$). Whatever may be $z_{\alpha\varepsilon}$ in the range 0 to l, $u(z)=\bar{u}(z_{\alpha\varepsilon\eta})$, $J_\varepsilon(z)=J_\varepsilon(z_{\alpha\varepsilon\eta})$, $S^*_{\alpha\varepsilon\eta}(z;\, n)=S^*_{\alpha\varepsilon\eta}(z_{\alpha\varepsilon\eta};\, n)$, $\kappa_{\alpha\varepsilon\eta}(z,\, z';\, n)=\kappa_{\alpha\varepsilon\eta}(z_{\alpha\varepsilon\eta},\, z_{\alpha\varepsilon\eta};\, n)$. Let us assume $\gamma_{\alpha\varepsilon}(z)=\gamma_{\alpha\varepsilon}(z_{\alpha\varepsilon\eta})$. Also in this case $S^*_{\alpha\varepsilon\eta eq}$ may be formally expressed by Eq. (18), provided that :

$$\chi_{\alpha\varepsilon\eta}(z_{\alpha\varepsilon};\, n) = \frac{\displaystyle\int_0^l\int_0^l \exp\left\{-\kappa_{\alpha\varepsilon\eta}(z_{\alpha\varepsilon\eta},\, z_{\alpha\varepsilon\eta};\, n)\,\frac{|z-z'|}{l}\right\}\psi_{\alpha 1}(z)\,\psi_{\alpha 1}(z')\,dzdz'}{\left[\displaystyle\int_0^l \psi_{\alpha 1}(z)\,dz\right]^2} \tag{22}$$

The closed form integration of Eq. (22) obviously depends on $\psi_{\alpha 1}(z)$. It is possible to verify, however, that in the class of the usual mode shapes a suitable $k_{\alpha\varepsilon\eta}$ value exists, depending on $\psi_{\alpha 1}(z)$, making Eq. (20) an almost exact approximation of Eq. (22). Table 1 gives a list of

Table 1 Noticeable values of $k_{\alpha\varepsilon\eta}$ for horizontal structures ($\phi=\pi/2$).

$\psi_{\alpha 1}(z)$	$k_{\alpha\varepsilon\varepsilon}$ ($\varepsilon=u,\ v,\ w,\ s$)	$k_{\alpha uw}$
1	0.50	0.50
$\sin(\pi z/l)$	0.39	0.38
$\sin(\pi z/2l)$	0.40	0.40
$[1-\cos(2\pi z/l)]/2$	0.32	0.31
$(z/l)^{0.5}$	0.44	0.44
$(z/l)^{1.0}$	0.38	0.38
$(z/l)^{1.5}$	0.33	0.33
$(z/l)^{2.0}$	0.29	0.29
$(z/l)^{2.5}$	0.26	0.26

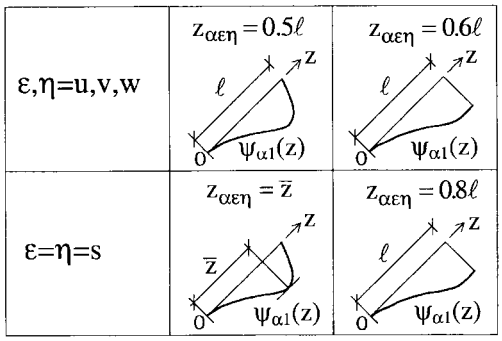

Fig. 2 Estimation criterion for $z_{\alpha\varepsilon\eta}$

$k_{\alpha\varepsilon\varepsilon}$, $k_{\alpha uw}$ values fulfilling this property; $k_{\alpha uv}$, $k_{\alpha vw}$ values are clearly insignificant due to the non-correlation of u', v' and v', w'.

In order to generalize this formulation to vertical ($\phi=0$) and inclined structures, an extensive parametric numerical analysis was carried out taking into account a wide class of $u(z)$, $J_\varepsilon(z)$, $\psi_{\alpha 1}(z)$, $S^*_{\alpha\varepsilon\eta}(z;\ n)$, $\kappa_{\alpha\varepsilon\eta}(z,\ z';\ n)$ functions. Assuming that $\gamma_{\alpha\varepsilon}$ is slightly dependent on z (however not changing its sign) and that $\psi_{\alpha 1}(z)\psi_{\alpha 1}(z')\geq 0$ for any couple of z, z' values in the range 0 to l, the results showed that, whatever the functions $u(z)$, $J_\varepsilon(z)$, $\psi_{\alpha 1}(z)$, $S^*_{\alpha\varepsilon\eta}(z;\ n)$, $\kappa_{\alpha\varepsilon\eta}(z,\ z';\ n)$ may be, a couple of $z_{\alpha\varepsilon\eta}$, $k_{\alpha\varepsilon\eta}$ values exists, called the reference coordinate and the equivalent correlation factor, making Eqs. (18) and (20) excellent approximations of Eqs. (16) and (17). These values main-

Table 2 Noticeable values of $k_{\alpha\varepsilon\varepsilon}$ for vertical structures ($\phi=0$).

$\psi_{\alpha 1}(z)$	$k_{\alpha\varepsilon\varepsilon}$ ($\varepsilon=u,\ v,\ w$)	$k_{\alpha ss}$
1	0.50	0.50
$\sin(\pi z/l)$	0.37	0.41
$\sin(\pi z/2l)$	0.40	0.38
$[1-\cos(2\pi z/l)]/2$	0.30	0.33
$(z/l)^{0.5}$	0.40	0.38
$(z/l)^{1.0}$	0.35	0.33
$(z/l)^{1.5}$	0.30	0.28
$(z/l)^{2.0}$	0.27	0.25
$(z/l)^{2.5}$	0.24	0.22

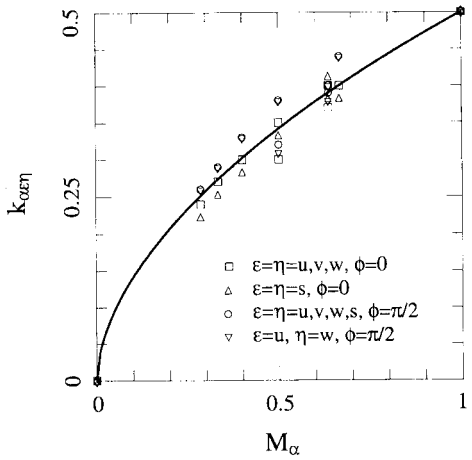

Fig. 3 Diagram of $k_{\alpha\varepsilon\eta}$

ly depend on the modal shape $\psi_{\alpha 1}(z)$, on the ε, η components of the excitation and on the ϕ angle. Fig. 2 provides an efficient criterion for estimating $z_{\alpha\varepsilon\eta}$. Table 2 collects a series of noticeable $k_{\alpha\varepsilon\varepsilon}$ values referred to vertical structures; $k_{\alpha ww}$ values are not relevant since vertical turbulence does not excite vertical structures (Eq. (7)).

The joint analysis of Tables 1 and 2 reveals the possibility of expressing $k_{\alpha\varepsilon\eta}$ by the following unitary formula :

$$k_{\alpha\varepsilon\eta} = 0.5 M_\alpha^{0.55} \tag{23}$$

$$M_\alpha = \frac{1}{\hat{\psi}_{\alpha 1} l} \int_0^l | \psi_{\alpha 1}(z) | dz \tag{24}$$

where $\hat{\psi}_{\alpha 1} = \max \{ | \psi_{\alpha 1}(z) | \}$ for z in the range 0 to l. Fig. 3 demonstrates the reliability of Eqs. (23) and (24) comparing their diagram with the $k_{\alpha\varepsilon\eta}$ values in Tables 1 and 2.

Eqs. (23) and (24) indicate the strict dependence of $k_{\alpha\varepsilon\eta}$ on the fundamental mode and, especially, its physical meaning. Increasing the distance of $\psi_{\alpha 1}(z)$ from the uniform shape reduces the structural portion where the load is effectively applied. This is equivalent to increasing the loading coherence as is clearly explained by the analysis of the following two limit cases.

When $\psi_{\alpha 1}(z)=1$, the whole structure is uniformly excited by wind that fully develops its coherence properties over all its length. In this case Eq. (22) is solved by Eq. (20) assigning $k_{\alpha\varepsilon\eta}=0.5$ (coherently with Eqs. (23) and (24) where $M_\alpha=1$).

In the theoretical case in which $\psi_{\alpha 1}(z)=\delta(z-\bar{z})$, where $\delta(\cdot)$ is the Dirac function and $\bar{z}$ belongs to the range 0 to l, wind loading practically acts only in the point $z=z$ becoming de facto identically coherent. The solution of Eq. (22) provides the result $\chi_{\alpha\varepsilon\eta}=1$ corresponding to Eq. (20) for $k_{\alpha\varepsilon\eta}=0$ (as correctly obtained applying Eqs. (23) and (24) when $M_\alpha=0$).

The GEST has the same conceptual meaning of the EWST (Solari 1988). When applying the actual wind loading process to the structure, the reduction effect due to the partial correlation is implicit in the coherence function defined by Eq. (13). Assuming the wind loading process as identically coherent in space, the same reduction effect is transferred into the spec-

tral density functions through the harmonic filter defined by Eq. (20). As it is shown in the next section, this filter reduces the high frequency range of the turbulence and the shedding frequency components of the wake excitation.

4. Numerical examples

To illustrate the application and the effectiveness of the GEST, three slender line-like prismatic structural models are examined.

All models are immersed in a wind field characterized by a mean velocity profile $u(z)=2.5u_*\ln(Z/z_0)$ with a roughness coefficient $z_0=0.7$ m; the shear velocity u_* varies in the range 0 to 3 m/s; $Z=h+z\cos\phi$. The turbulence is schematized by the model proposed by Solari and Piccardo (1998).

The reduced psdf of the u', v', w' turbulence components is expressed by the relationship :

$$nS^*_{\alpha\varepsilon\varepsilon}(z\,;n)=\frac{nS_{\varepsilon\varepsilon}(z\,;n)}{\sigma^2_\varepsilon(z)}=\frac{d_\varepsilon nL_\varepsilon(z)/\bar{u}(z)}{[1+1.5d_\varepsilon nL_\varepsilon(z)/\bar{u}(z)]^{5/3}}\quad(\varepsilon=u\,,\,v\,,\,w) \tag{25}$$

where $S_{\varepsilon\varepsilon}$ is the psdf of ε'; $d_u=6.868$, $d_v=d_w=9.434$; $\sigma^2_\varepsilon=\beta_\varepsilon u_*^2$ is the variance of ε', $\beta_u=4.96$, $\beta_v=2.79$, $\beta_w=1.24$; L_ε is the integral length scale of the ε turbulence component in the x direction, $L_u(z)=300(z/200)^{0.65}$ (L_u, z in m), $L_v(z)=0.25\,L_u(z)$, $L_w(z)=0.10\,L_u(z)$.

The reduced cpsdf of u', w' is expressed by :

$$nS^*_{\alpha uw}(z\,;n)=\frac{nS_{uw}(z\,;n)}{\sigma_u(z)\sigma_w(z)}=\frac{\rho_{uw}(z)}{A_{uw}(z)}\,\frac{\sqrt{nS^*_{\alpha uu}(z\,;n)}\sqrt{nS^*_{\alpha ww}(z\,;n)}}{\sqrt{1+0.4[nL_u(z)/u(z)]^2}} \tag{26}$$

where S_{uw} is the cpsdf of u', w'; $\rho_{uw}=-1/\sqrt{\beta_u\beta_w}=-0.40$ is the cross-correlation coefficient of u', w'; $A_{uw}(z)=[L_w(z)/L_u(z)]^{0.17}=0.68$.

The coherence function of the u', v', w' turbulence components is given by Eq. (13) assuming :

$$\kappa_{\alpha\varepsilon\eta}(z\,,z'\,;n)=\frac{2nC_{z\varepsilon\eta}l}{\bar{u}(z)+u(z')}\quad(\varepsilon,\,\eta=u\,,\,v\,,\,w) \tag{27}$$

where $C_{z\varepsilon\eta}=\sqrt{C^2_{Y\varepsilon\eta}\sin^2\phi+C^2_{Z\varepsilon\eta}\cos^2\phi}$ is the exponential decay factor of the ε, η components of the turbulence along z; $C_{Y\varepsilon\eta}$, $C_{Z\varepsilon\eta}$ are the exponential decay factors of the ε, η turbulence components in the Y and Z directions; $C_{Yuu}=C_{Zuu}=10$, $C_{Yuw}=8.25$, $C_{Yvv}=C_{Yww}=C_{Zvv}=C_{Zuw}=6.5$, $C_{Zww}=3$.

The reduced psdf of the wake excitation is given by the relationship (Vickery and Clark 1972) :

$$nS^*_{\alpha ss}(z\,;n)=\frac{n/n_{\alpha s}(z)}{\sqrt{\pi}B(z)}\exp\left\{-\left[\frac{1-n/n_{\alpha s}(z)}{B(z)}\right]^2\right\} \tag{28}$$

where $n_{\alpha s}(z)=S_{Y\alpha}u(z)/b$ is the α component of the shedding frequency; S is the Strouhal number;

Υ_x=2, Υ_y=1; Υ_θ depends on the shape of the cylinder; $B(z)=\sqrt{B_0^2+2I_u^2(z)}$ is the bandwidth spectral parameter, B_0=0.08.

The wake coherence function is given by Eq. (13) assuming (ESDU 1990b):

$$\kappa_{\alpha s s}(z, z'; n)=\frac{1}{L}\frac{l}{b} \tag{29}$$

where L is the correlation length (in b's) of the vortex shedding.

Model 1 represents an r.c. chimney (ϕ=0, h=0) l=180 m high; its diameter is b=5.6 m; the mass per unit height is m=10686 kg/m. The x alongwind and y crosswind fundamental frequencies are $n_{x1}=n_{y1}$=0.26 Hz. The related mode shapes are $\psi_{x1}(z)=\psi_{y1}(z)=(z/l)^{\zeta}$, ζ=2.15. The damping factors are $\xi_{x1}=\xi_{y1}$=0.005. The aerodynamic coefficients are : c_d=0.8, $c_l=c_m$=0; $c_d'=c_l'=c_m'=0$; $\tilde{c}_{ds}$=0, $\tilde{c}_{ls}$= 0.2, $\tilde{c}_{ms}$=0; S=0.2, L=1. Using the criterion in Fig. 2, $z_{\alpha\varepsilon\eta}$=108 m ($\varepsilon$, η=u, v, w), $z_{\alpha ss}$=144 m (α=x, y). By means of Eqs. (23) and (24), $k_{\alpha\varepsilon\eta}$=0.2660 ($\varepsilon$, η=u, v, w, s; α=x, y).

Model 2 is an inclined (ϕ=π/4) square section steel element whose lower extreme lies h=20 m over the ground; it is l=30 m long; its side is b=0.4 m; the mass per unit length is m=444.6 kg/m; the mass moment of inertia per unit length is I=62.87 kgm; $n_{x1}=n_{y1}$=1.5 Hz; $\psi_{x1}(z)=\psi_{y1}(z)=\sin(\pi z/l)$; $\xi_{x1}=\xi_{y1}$=0.005. The torsional fundamental frequency, mode shape and damping factor are $n_{\theta 1}$=30 Hz, $\psi_{\theta 1}(z)=[1-\cos(2\pi z/l)]/2$, $\xi_{\theta 1}$=0.01. The aerodynamic coefficients are : c_d=1.2, $c_l=c_m$=0; c_d'=0, c_l'=-3.2, c_m'=0.5; $\tilde{c}_{ds}$=0, $\tilde{c}_{ls}$=0.5, $\tilde{c}_{ms}$=0.025; S=0.1, L=1, Υ_θ=0.9. Using Fig. 2 and Eqs. (23) and (24), $z_{\alpha\varepsilon\eta}$=15 m ($\alpha$=$x$, y, θ), $k_{x\varepsilon\eta}=k_{y\varepsilon\eta}$=0.3900, $k_{\theta\varepsilon\eta}$=0.3415 ($\varepsilon$, η=u, v, w, s).

Model 3 represents a horizontal bridge (ϕ=π/2) at height h=20 m; its length is l=100 m; the width and the thickness are respectively 11.5 m and 2.6 m, this latter value being assumed as the reference b size; the mass and the mass moment of inertia per unit length are m= 13000 kg/m and I=188000 kgm; n_{x1}=0.3 Hz, n_{y1}=0.5 Hz, $n_{\theta 1}$=1 Hz; $\psi_{x1}(z)=\psi_{y1}(z)=\sin(\pi z/l)$, $\psi_{\theta 1}(z)=[1-\cos(2\pi z/l)]/2$; $\xi_{x1}=\xi_{y1}=\xi_{\theta 1}$=0.005. The aerodynamic coefficients are : c_d=1, c_l=-2.5, c_m=0; c_d'=0, c_l'=33, c_m'=20; $\tilde{c}_{ds}$=0, $\tilde{c}_{ls}$=0.35, $\tilde{c}_{ms}$=0.02; S=0.12, L=1, Υ_θ=0.9. Using Fig. 2 and Eqs. (23) and (24), $z_{\alpha\varepsilon\eta}$=50 m ($\alpha$=$x$, y, θ), $k_{x\varepsilon\eta}=k_{y\varepsilon\eta}$=0.3900, $k_{\theta\varepsilon\eta}$=0.3415 ($\varepsilon$, η=u, v, w, s).

Matrices [c] (Eq. (7)) define the role of the different excitatory components (ε, η=u, v, w, s) with reference to the structural components of the response (α=x, y, θ) (Piccardo and Solari 1996a).

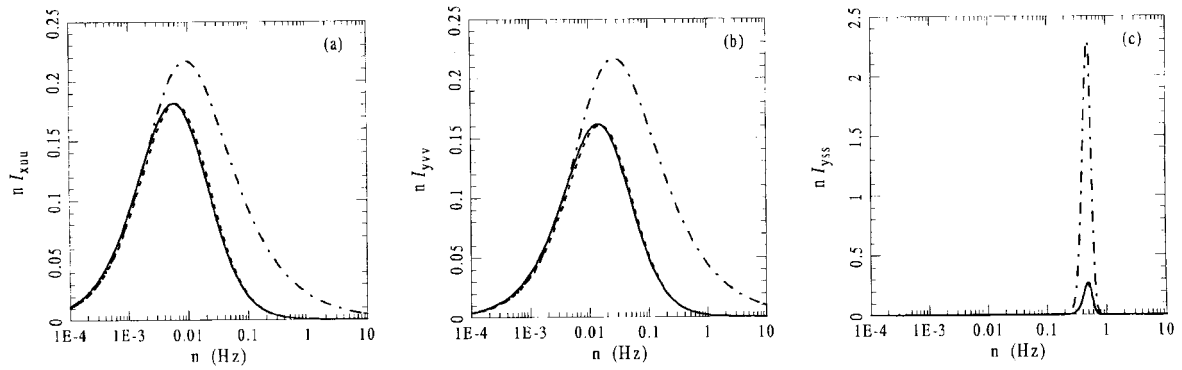

Fig. 4 $nI_{\alpha\varepsilon\eta}$ diagrams for model 1

Due to its polar symmetry and vertical axis, model 1 is excited by the u' longitudinal turbulence in the x alongwind direction and by the v' lateral turbulence and s' vortex shedding in the y crosswind direction. No loading mechanism excites the θ torsional motion.

Since model 2 is inclined and xz is a symmetry plane, it is excited by u' in the x alongwind direction and by v', w', s' in the y crosswind and θ torsional generalized directions.

Model 3 is horizontal with the yz as a symmetry plane; it is excited by u', w' in the x alongwind direction, by u', w', s' in the y crosswind direction and by w', s' in the θ torsional direction; θ is not excited by u' due to the assumption c_m=0.

Figs. 4, 5, 6, referred to models 1, 2, 3, respectively, show all the meaningful diagrams of

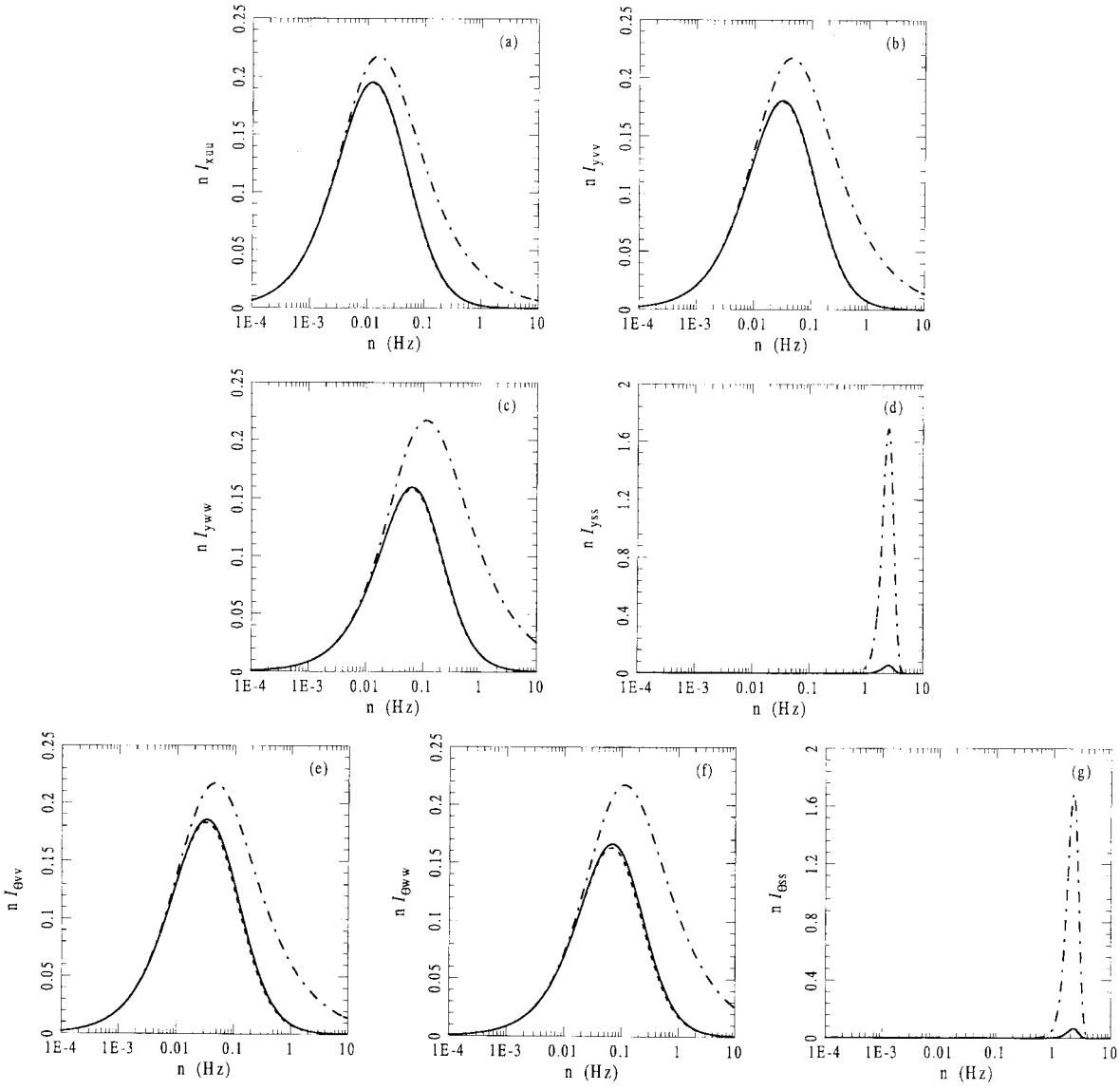

Fig. 5 $nI_{\alpha\varepsilon\eta}$ diagrams for model 2

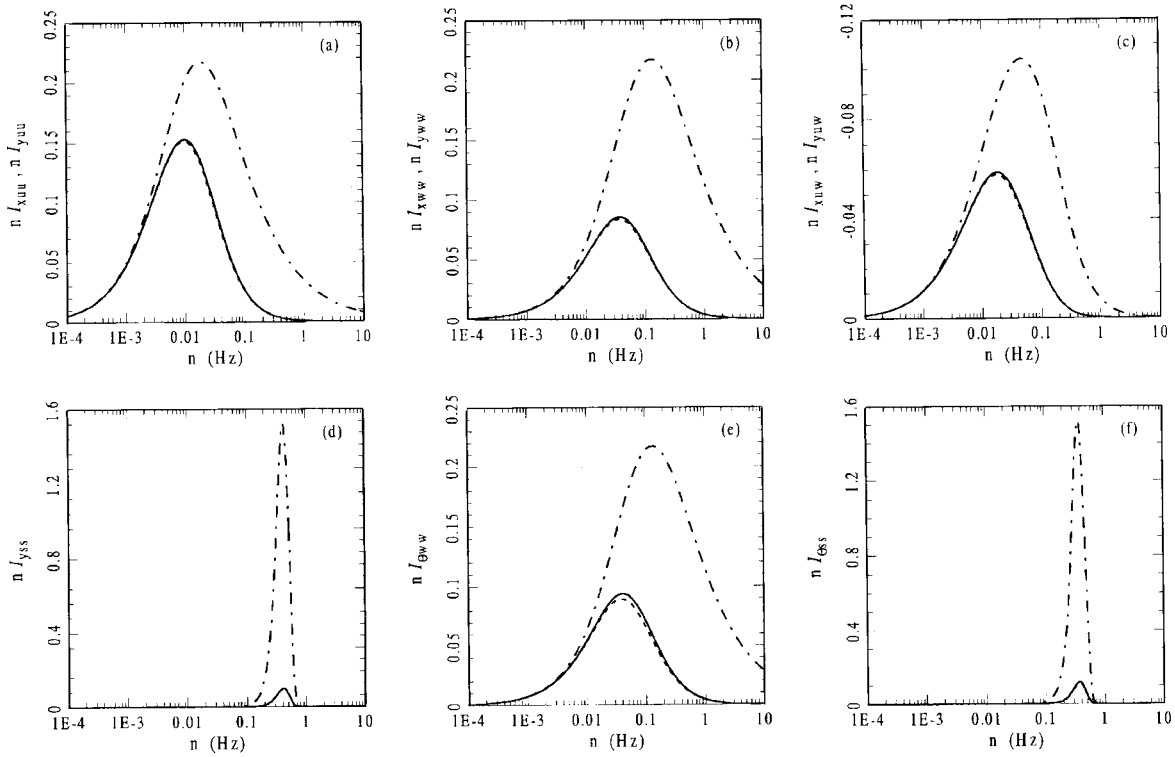

Fig. 6 $nI_{\alpha\varepsilon\eta}$ diagrams for model 3

$nI_{\alpha\varepsilon\eta}$ (α=x, y, θ; ε, η=u, v, w, s) for u_*=1 m/s.

The dot-dashed lines correspond to the ideal case $\mathrm{Coh}_{\alpha\varepsilon\eta}(z, z'; n)=1$, $I_{\alpha\varepsilon\eta}(n)=S^*_{\alpha\varepsilon\eta}(z_{\alpha\varepsilon\eta}; n)$ (A). The solid lines represent the actual situation (Eq. (16)) (B). The dashed lines denote the use of the GEST (Eqs. (17), (18), (20)) (C). The almost perfect superposition between (B) and (C) diagrams highlights the precision of this method. The comparison between (A) and

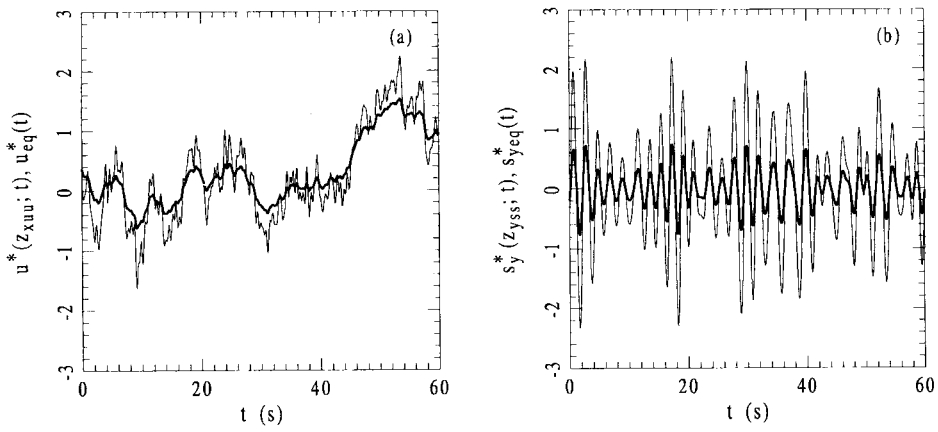

Fig. 7 Sample time-histories (model 1)

(C) diagrams points out the role of the harmonic filter $\chi_{\alpha\varepsilon\eta}$ (Eq. (20)) that multiplied by $S^*_{\alpha\varepsilon\eta}$ gives rise to $S^*_{\alpha\varepsilon\eta\, eq}$ (Eq. (18)).

As a further example of the role of the filter $\chi_{\alpha\varepsilon\eta}$, Fig. 7a shows two pieces of sample time-histories, $u^*(z_{xuu}; t)$ and $u^*_{eq}(t)$, derived from $S^*_{xuu}(z_{xuu}; t)$ and $I_{xuu}(n)=S^*_{xuu\, eq}(n)$. Fig. 7b shows two pieces of sample time-histories, $s^*_y(z_{yss}; t)$ and $s^*_{y\, eq}(t)$, derived from $S^*_{yss}(z_{yss}; n)$ and $I_{yss}(n)=S^*_{yss\, eq}(n)$. Thin lines correspond to the actual reduced processes; thick lines correspond to the reduced equivalent ones. All functions are referred to the model 1 and are derived by the random phase method (Shinozuka and Jan 1972) using a time step Δt=0.1 s and a duration T=600 s.

With reference to Fig. 7a one sees that the filtering effect of χ_{xuu} mainly reduces the high frequency harmonic content of the longitudinal turbulence (Fig. 4a). This explains the better regularity of the thick line in comparison with that of the thin line.

With reference to Fig. 7b, on the other hand, one sees that the filtering effect of χ_{yss} reduces the shedding frequency content of the wake excitation (Fig. 4c). It follows that the

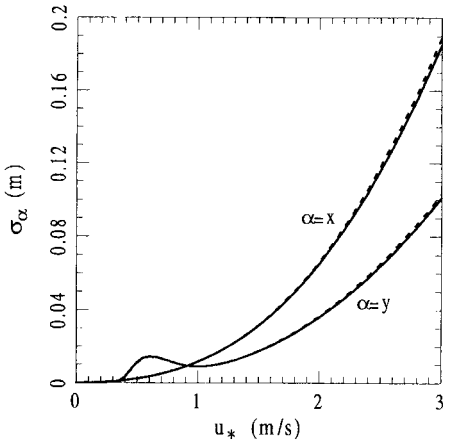

Fig. 8 Dynamic response of model 1

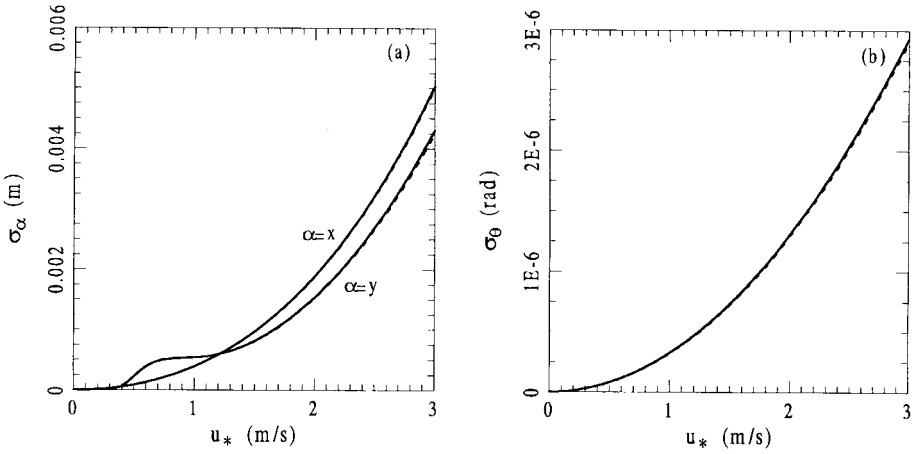

Fig. 9 Dynamic response of model 2

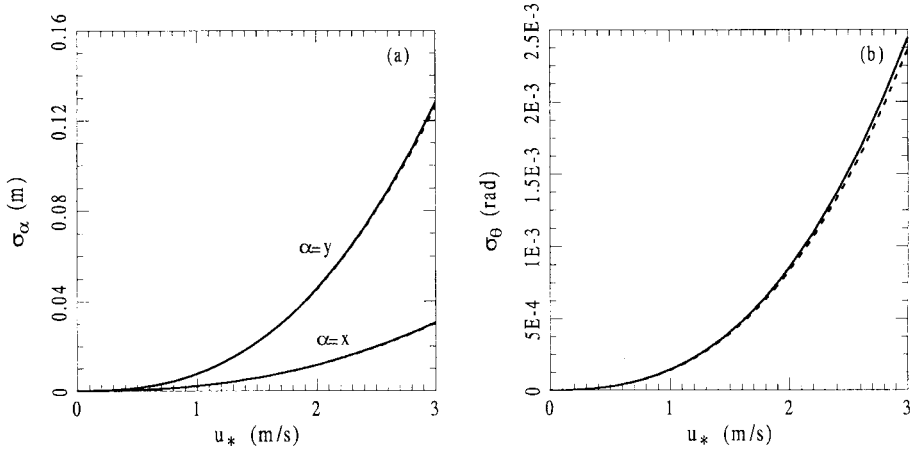

Fig. 10 Dynamic response of model 3

thick line retains the shape of the thin line with lower amplitudes.

The dynamic alongwind, crosswind and torsional response of models 1, 2 and 3 is calculated using the method proposed by Piccardo and Solari (1998).

Fig. 8 shows the rms values of the x alongwind and y crosswind displacements at the top of model 1. Figs. 9 and 10 show the rms values of the x alongwind and y crosswind displacements and of the θ torsional rotation of models 2 and 3 in the middle of their spans. The solid lines correspond to the rigorous solutions based on Eq. (16); the dashed lines are the results obtained applying the GEST (Eqs. (17), (18), (20)). The superposition of the solid and dashed diagrams enhances the precision of the method.

5. Conclusions and perspectives

Using the Generalized Equivalent Spectrum Technique proposed in this paper, the external fluctuating forces are schematized by equivalent identically coherent processes, rather than by the actual multi-dimensional processes. The set of these processes is identified by a cross-power spectral density function, the Generalized Equivalent Spectrum, whose expression is given in closed form. It is demonstrated that the use of this method leads to almost exact solutions of the 3-D wind-excited response of slender structures and structural elements with negligible computational burdens.

The authors of this paper are at present working to generalize the above method to three-dimensional structures.

References

Davenport, A.G. (1961), "The application of statistical concepts to wind loading of structures", *Proc. Instn. Civ. Engrs.* **19**, 449-472.

Di Paola, M. (1998), "Digital simulation of wind field velocity", *J. Wind Engng. Ind. Aerod.*, in press.

Engineering Sciences Data Unit (1990a), "Circular-cylindrical structures : dynamic response to vortex shedding. Pt 1 : Calculation procedures and derivation", *ESDU Item 85038*, London, England.

Engineering Sciences Data Unit (1990b), "Characteristics of atmospheric turbulence near the ground. Part II : Single point data for strong winds (neutral atmosphere)", *ESDU Item 85020*, London, Eng-

land.
Piccardo, G. & G. Solari (1996a), "A refined model for calculating 3-D equivalent static wind forces on structures", *J. Wind Engng. Ind. Aerod.*, **65**, 21-30.
Piccardo, G. & G. Solari (1996b), "Equivalent wind loading spectrum technique", *Proc., 3rd Europ. Conf. On Struct. Dyn.*, Florence, Balkema, Rotterdam, 213-220.
Piccardo, G. & G. Solari (1998), "3-D wind excited response of slender structures : Basic formulation, closed form solution, applications", submitted for possible publication in the *J. Struct. Engng., ASCE.*
Shinozuka, M. & C.M. Jan (1972), "Digital simulation of random processes and its applications", *J. Sound Vibr.*, **25**(1), 111-128.
Solari, G. (1985), "Mathematical model to predict 3-D wind loading on buildings", *J. Engng. Mech., ASCE*, **111**, 254-276.
Solari G. (1988), "Equivalent wind spectrum technique : theory and applications", *J. Struct. Engng., ASCE*, **114**, 1303-1323.
Solari, G. (1994), "Gust-excited vibrations of structures", In Sockel, H. Ed., *Wind-excited vibrations of structures*, Springer-Verlag, Wien, 195-291.
Solari, G. & G. Piccardo (1998), "Probabilistic 3-D turbulence modeling for gust buffeting", to be submitted for publication.
Vellozzi, J. & E. Cohen (1968), "Gust response factor", *J. Struct. Div., ASCE.* **97**, 1295-1313.
Vickery, B.J. & W. Clark (1972), "Lift or across-wind response of tapered stacks", *J. Struct. Division, ASCE.* **98**, 1-20.